

A Bayesian Approach to Classifying Supernovae With Color

Natalia Connolly¹, Brian M. Connolly²

November 2, 2018

ABSTRACT

Upcoming large-scale ground- and space- based supernova surveys will face a challenge identifying supernova candidates largely without the use of spectroscopy. Over the past several years, a number of supernova identification schemes have been proposed that rely on photometric information only. Some of these schemes use color-color or color-magnitude diagrams; others simply fit supernova data to models. Both of these approaches suffer a number of drawbacks partially addressed in the so-called Bayesian-based supernova classification techniques. However, Bayesian techniques are also problematic in that they typically require that the supernova candidate be one of a known set of supernova types. This presents a number of problems, the most obvious of which is that there are bound to be objects that do not conform to any presently known model in large supernova candidate samples. We propose a new photometric classification scheme that uses a Bayes factor based on color in order to identify supernovae by type. This method does not require knowledge of the complete set of possible astronomical objects that could mimic a supernova signal. Further, as a Bayesian approach, it accounts for all systematic and statistical uncertainties of the measurements in a single step. To illustrate the use of the technique, we apply it to a simulated dataset for a possible future large-scale space-based Joint Dark Energy Mission and demonstrate how it could be used to identify Type Ia supernovae. The method's utility in pre-selecting and ranking supernova candidates for possible spectroscopic follow-up – *i.e.*, its usage as a supernova trigger – will be briefly discussed.

Subject headings: supernovae: general – techniques: photometric

¹Physics Department, Hamilton College, Clinton, NY 13323, USA; nconnoll@hamilton.edu

²Department of Physics and Astronomy, University of Pennsylvania, Philadelphia, PA 19104-6396, USA; brianco@sas.upenn.edu

1. Introduction

In recent years, the question of photometric identification of supernova candidates has emerged as one of the crucial issues to be resolved before the advent of large-space supernova cosmology experiments, both ground-based (*e.g.*, the Large Synoptic Survey Telescope [LSST], the Dark Energy Survey [DES], the Panoramic Survey Telescope and Rapid Response System [Pan-STARRS]), and space-based (*e.g.*, the *Joint Dark Energy Mission* [JDEM]). There are a number of reasons for this. First, although there have been some interesting developments in the possible uses of supernova other than Type Ia for cosmology (Baron et al. 2004; Hamuy and Pinto 2002; Nugent 2006; Poznanski et al. 2009), Type Ia supernovae (SNIa) remain the staple of experimental cosmology. Second, SNe Ia are most reliably identified using spectroscopy due to the presence of a characteristic SiII line at 6150 Å in the supernova rest frame. However, future large ground-based surveys are expected to collect thousands of supernova candidates, making a spectroscopic follow-up of each candidate all but unrealistic. The identification of supernova candidates (with possible spectroscopic follow-up for a select sample) based on broadband photometry remains the only feasible alternative.

There have been a number of methods proposed to identify supernovae using broadband photometry that can be divided into three broad categories. One includes methods that rely on color-color or color-magnitude diagrams (Poznanski et al. 2002; Riess et al. 2004; Johnson and Crofts 2005; Sullivan et al. 2006a). It is also possible to fit supernova data to models, and select the best fit (using, for example, a χ^2), which can be used to represent the supernova type (Jha et al. 2007; Guy et al. 2007; Conley et al. 2008). Finally, the third category involves recently developed techniques based on a probabilistic (Bayesian) approach to the problem (Kuznetsova and Connolly 2007; Poznanski et al. 2007). The method proposed in this work, although closer in spirit to the second category, has a number of advantages over both.

The existing techniques, while adequate in many cases, have a number of serious shortcomings. For example, supernova identification schemes based on color-color and color-magnitude diagrams involve comparing the colors and/or magnitudes of a given supernova candidate with what is predicted by various supernova models. This is an intuitive approach, allowing one to visually judge the goodness of fit of the data to the models; however, it is difficult to account for all statistical and systematic uncertainties in a single step.

A class of techniques that could be generally described as “ χ^2 -based” simply find the best fit for a given supernova candidate’s light curves to a supernova model. This is also an intuitive and often completely reasonable approach, which nevertheless suffers the following disadvantages:

1. “This object is not a supernova of any kind” is not a well-defined hypothesis in this as in any other frequentist approach (Edwards 1992).
2. Conversely, if the data happen to have large uncertainties, there is the possibility that a number of supernova models will be good fits to the data. There is no formalism to compute not only the probability that a given fit is good, but also that it is bad. In other words, what one is interested in is the posterior probability, the probability that a given hypothesis is true given the data. Calculating this probability requires that the probability that this hypothesis is false be also known.
3. Using a χ^2 -based technique only gives the information about the best fit for a given set of data to a model, while any information about worse fits is lost. The best fit will not necessarily reflect the true properties of the supernova.
4. In cases where one would like to use a tail probability for accepting or rejecting given supernova candidates (*e.g.*, as SNe Ia), the probability of falsely rejecting the null hypothesis (the so called Type I error rate) can be shown to be severely underestimated (see Sellke, Bayarri, & Berger (2001) and references therein).

Bayesian classification schemes address many of the problems of the above-mentioned methods. However, existing Bayesian-based supernova typing methods have a serious drawback: they require the knowledge of the complete set of objects that a supernova candidate might conceivably be (Kuznetsova and Connolly 2007; Poznanski et al. 2007). That is, they assume that a supernova candidate can only be one of a finite set of supernova types. However, even with the current small high-redshift SN sample (obtained almost exclusively with the Hubble Space Telescope) one occasionally finds supernova candidates with surprising new properties that do not seem to conform to any known models (Barbary et al. 2009). Problems with assuming a finite set of supernova-like objects are further addressed in Section 3.4.

In our work, we introduce a likelihood ratio (a Bayes factor) that is capable of discriminating between SNe Ia and *anything else* based on broadband photometric measurements. The most important feature of this technique is that it is independent of the knowledge of the complete set of objects that a supernova candidate might conceivably be. Another advantage is that, as with all Bayesian-based techniques, this method allows one to include all possible statistical and systematic uncertainties in a single step. Finally, the Bayes factor is formulated in terms of color and thus does not require that one make any assumptions about the absolute magnitudes of the supernova candidates in the broadband filters used. Of course it is often desirable to include magnitudes in the formalism; however, not only does it require making assumptions about the distribution of magnitudes for various known

supernova types, but also it places a hard upper limit on the intrinsic magnitudes of objects that have yet to be observed. But more importantly, “anomalous” (non-supernova) objects can be defined in a far more mathematically elegant and computationally manageable way using color alone.

The Bayes factor is defined as

$$\mathcal{R} = P(\text{Phot}|\text{Ia})/P(\text{Phot}|\text{non-Ia}). \quad (1)$$

where $P(\text{Phot}|\text{Ia})$ is the probability of obtaining the observed photometry (colors) from a SN Ia, and $P(\text{Phot}|\text{non-Ia})$ is the probability of obtaining the data for any other object (which could be a non-SN Ia or any other object capable of mimicking an SN Ia signal). Both probabilities take into account the *relative* distribution of light among the broadband filters used for the measurements. In general, no specific set of models (or templates) for non-SNe Ia is required for the calculation of the denominator.

On a more technical note, it is worthwhile to point out that Bayes factors are normally used for deciding on the best of two hypotheses. This allows one to easily set thresholds on the Bayes factor in terms of the so-called Type I and Type II error rates¹ in the same way as thresholds are set on the likelihood ratio in Wald (1945, 1947). Also, although the main focus of this work is to describe a method that can identify SNe Ia, the Bayes factor can be easily cast in terms of a posterior probability that a candidate is a Type T supernova, where T could be Ibc, II-P, II-n, *etc.*²

This paper is organized as follows. In Section 2 we derive an expression for \mathcal{R} for a

¹Type I error is the probability of rejecting the null hypothesis when the null hypothesis is in fact correct; it is thus a measure of the purity of the selection. Type II error is the probability that the null hypothesis will be accepted when the null hypothesis is in fact false; it is thus a measure of the efficiency of the selection

²Consider some data D , a hypothesis \mathcal{H}_0 , and its alternative \mathcal{H}_1 . The Bayes factor can be defined as

$$\mathcal{R} = \frac{P(D|\mathcal{H}_1)}{P(D|\mathcal{H}_0)}. \quad (2)$$

The posterior probability that the alternative hypothesis is true for the data can then be written in terms of \mathcal{R} provided that one knows the priors for \mathcal{H}_0 and \mathcal{H}_1 , denoted by $P(\mathcal{H}_0)$ and $P(\mathcal{H}_1)$, respectively:

$$P(\mathcal{H}_1|D) = \frac{\mathcal{R} \frac{P(\mathcal{H}_1)}{P(\mathcal{H}_0)}}{\mathcal{R} \frac{P(\mathcal{H}_1)}{P(\mathcal{H}_0)} + 1}. \quad (3)$$

See Berger and Pericchi (2001) for details. Although there are historical reasons why the Bayes factor is formulated in this way, it is also convenient when setting thresholds for the error rates because often the errors rates are at least somewhat determined by the information contained in the priors on \mathcal{H}_0 and \mathcal{H}_1 .

number of different cases. We describe the performance of the method in Section 3. Section 4 presents a discussion of the results.

2. Derivation of the Bayes Factor

2.1. Overview of the Calculation

The Bayes factor, \mathcal{R} , introduced above, is defined as the probability of obtaining the photometric measurements assuming that the supernova candidate is a Type Ia over the probability that it is anything else. In practice, the probability that a candidate is an SN Ia is the probability that the colors are consistent with what is expected for an SN Ia using some prior knowledge about the behavior of Type Ia’s. In our first formulation of the Bayes factor, if the candidate is not in fact an SN Ia, then the distribution of light in the broadband filters used can be arbitrary. However, one could argue that much of the background for SNe Ia will be supernovae of other types whose behavior is relatively well-known. However, the unprecedented scale of the future supernova surveys makes it highly likely that many new types of transient objects will be discovered. Also, little is known about the *rates* of non-Type Ia supernovae, especially at very high redshifts, making it difficult to predict the behavior of the background at those redshifts.

We begin with a general overview of the calculation of \mathcal{R} . For simplicity, we assume that there are only two broadband filters, and that there is a single measurement of the supernova candidate’s flux in each. Suppose that the flux is measured in photon counts, and that M_1 counts are measured in the first filter, and M_2 , in the second. Further suppose that there exists a model (a template) for the behavior of SNe Ia in these filters, and that the model predicts that some mean fraction of photons, \bar{f} , must end up in the first filter, and $1-\bar{f}$, in the second. The numerator of \mathcal{R} , $P(\text{Phot}|\text{Ia})$, is essentially the probability that the measurement is consistent with this model. Assuming Poisson statistics for the photon distributions, it can be easily shown that $P(\text{Phot}|\text{Ia})$ takes the form of a standard binomial distribution:

$$P(\text{Phot}|\text{Ia}) = \binom{M_1 + M_2}{M_1} \bar{f}^{M_1} (1 - \bar{f})^{M_2}.$$

For the calculation of the denominator of \mathcal{R} , $P(\text{Phot}|\text{non-Ia})$, we do not make any *a priori* assumptions about the fraction of light that will end up in either filter. The Bayesian framework of the calculation allows one to circumvent this difficulty by marginalizing, or

integrating over, all possible fractions. Mathematically,

$$P(\text{Phot}|\text{non-Ia}) = \int_0^1 df \binom{M_1 + M_2}{M_1} f^{M_1} (1 - f)^{M_2}.$$

In reality, the calculation becomes rather more complicated. To begin with, the measured flux will most likely be better described using Gaussian, rather than Poisson, statistics. We must also allow for the possibility of multiple measurements and more than 2 filters. In the next section we will make the calculation more explicit and account for all of these factors.

2.2. Mathematical Details

Before we plunge into the full derivation of \mathcal{R} for the case of Gaussian statistics and multiple measurements and filters, we take a closer look at the simple case of a single measurement of a supernova candidate in just two filters, assuming that the photon count fluctuations in the filters are Poisson. Recall that we assume that M_1 counts are measured by the first filter and M_2 by the second; and that we have a model that predicts a certain fraction of photons, \bar{f} , for the first filter, and $(1 - \bar{f})$, for the second.

Following a similar derivation in Jeffreys (1961), let us now introduce two variables, f and b , such that the mean number of photons in the first filter is given by fb , and the mean number of photons in the second filter is given by $(1 - f)b$. Variable b ranges from 0 to ∞ , and can be thought of as the mean number of photons that are counted in both filters for a given measurement. Variable f ranges from 0 to 1, and can be thought of as the probability that the photons will end up in the first filter as opposed to the second. An analogy would be collecting balls into two receptor bins with different volumes: in this case, b would be the mean number of balls that will enter both bins, and f is the relative “acceptance” of one bin. The introduction of these variables allows us to expand the Bayes factor, Eqn. 1, in terms of f and b :

$$\mathcal{R} = \frac{\int_0^\infty db P(\text{Phot}|b, \text{Ia}) P(b|\text{Ia})}{\int_0^1 df \int_0^\infty db P(\text{Phot}|f, b, \text{non-Ia}) P(f, b|\text{non-Ia})}. \quad (4)$$

Here, the first term in the numerator, $P(\text{Phot}|b, \text{Ia})$, is the likelihood of obtaining the measurement given that the mean number of photons was measured to be $\bar{f}b$ in the first filter, and $(1 - \bar{f})b$ in the second. Likewise, the first term in the denominator, $P(\text{Phot}|f, b, \text{non-Ia})$, is the likelihood of obtaining the measurement given that the mean number of photons was

measured to be fb in the first filter, and $(1 - f)b$ in the second. Note that the numerator is not a function of f because f is single valued in the numerator, $f = \bar{f}$. If the photon distribution is governed by Poisson statistics, then:

$$P(\text{Phot}|b, \text{Ia}) = \frac{(\bar{f}b)^{M_1} e^{-\bar{f}b}}{M_1!} \frac{((1 - \bar{f})b)^{M_2} e^{-(1-\bar{f})b}}{M_2!}. \quad (5)$$

and

$$P(\text{Phot}|f, b, \text{non-Ia}) = \frac{(fb)^{M_1} e^{-fb}}{M_1!} \frac{((1 - f)b)^{M_2} e^{-(1-f)b}}{M_2!}. \quad (6)$$

The terms $P(b|\text{Ia})$ in the numerator and $P(f, b|\text{non-Ia})$ in the denominator of Eqn. 4, are prior probabilities containing information regarding the expected distribution of light in the two filters for an SN Ia and anything else, respectively. Defining b_{min} and b_{max} as the minimum and maximum bounds for b and assuming each value for b in between these bounds is equally probable, we have:

$$P(b|\text{Ia}) = \frac{1}{b_{max} - b_{min}}. \quad (7)$$

Note that the range of b will always be assumed to be $b = [0, \infty]$, although the upper and lower bounds will initially be set to b_{max} and b_{min} , respectively.³ However, if the candidate is not an SN Ia, we do not make any assumptions about what to expect, and so:

$$P(f, b|\text{non-Ia}) = \frac{1}{(b_{max} - b_{min})(f_{max} - f_{min})} = \frac{1}{b_{max} - b_{min}}. \quad (8)$$

as the upper (f_{max}) and lower (f_{min}) bounds of f are 1 and 0, respectively.

Note that $P(b|\text{Ia})$ and $P(f, b|\text{non-Ia})$ are *improper priors* (in other words, they assume probability density functions that are flat and are integrated from zero to infinity). This is not a major issue for our calculation because the priors happen to cancel. However, in general the use of improper priors must be treated with caution (Berger and Pericchi 2001). It is therefore important to check that \mathcal{R} does indeed behave properly; this will be addressed further in Section 3.2.

³Here we have adopted Jaynes' methodology (Jaynes and Bretthorst 2003), expressing the prior probabilities in terms of variables representing the bounds of those variables. These bounds are inserted at the end of the calculations (integrations) with the goal of avoiding handling variables whose limits are defined as $[0, \infty)$ – *i.e.*, to avoid priors whose probabilities approach 0.

With these priors, Eqn. 4 becomes:

$$\mathcal{R} = \frac{\binom{M_1+M_2}{M_1} \bar{f}^{M_1} (1 - \bar{f})^{M_2}}{\frac{1}{M_1+M_2+1}}. \quad (9)$$

In the calculation of Eqn. 9 b is effectively unconstrained, leaving the supernova candidate’s magnitude free to take on any value. That is, as we are only concerned with the relative fraction of photons in each filter (*i.e.*, color), we need not make any assumptions about the behavior of b .

We would now like to derive an equation analogous to Eqn. 9, but for the case of Gaussian statistics. Let us suppose that instead of measuring M_1 photons in the first filter and M_2 in the second, we now measure a flux F_1 in the first filter with an error σ_1 , and a flux F_2 in the second filter with an error σ_2 . As before, we parametrize the mean (or “true”) fluxes in the two filters as fb and $(1 - f)b$, and expand \mathcal{R} in terms of f and b , leading to Eqn. 4. We then simply replace the Poisson distributions with Gaussian ones using the usual notation for a Gaussian distribution, $G(x; \mu, \sigma) = \frac{1}{\sqrt{2\pi}\sigma} e^{-\frac{(\mu-x)^2}{2\sigma^2}}$. Equation 4 becomes

$$\mathcal{R} = \frac{\int_0^\infty db G(F_1; \bar{f}b, \sigma_1) G(F_2; (1 - \bar{f})b, \sigma_2)}{\int_0^1 df \int_0^\infty db G(F_1; fb, \sigma_1) G(F_2; (1 - f)b, \sigma_2)}. \quad (10)$$

The integration over b in Eqn. 10 can be reduced further leading to the appearance of the Gauss error function. However, the integration over f in the denominator can only be done numerically.

We now make Eqn. 10 even more realistic by considering multiple measurements (say, N) and an arbitrary number of filters (say, M). Using the formalism we have developed above, we will assume that for the j^{th} measurement the fraction of light in the k^{th} filter is f_j^k , and the total light distributed between all the filters and all the measurements is given by b . Therefore, the hypothesized flux in the k^{th} filter and j^{th} measurement is given by $f_j^k b$. Again, if the supernova is assumed to be a Type Ia, then we have a model that describes the fraction of light in each of the filters for each of the measurements must be. The model must take into account the many possible observational parameters that characterize an SN Ia. For example, it is known that SNe Ia have a variety of possible “stretch” values, which parametrize the width of their light curves (Perlmutter et al. 1997). Following the approach used in Kuznetsova and Connolly (2007), we represent the Type Ia supernova parameters by $\vec{\theta}$, defined as

$$\vec{\theta} \equiv (s, A_v, R_v, t_{diff}, z). \quad (11)$$

where s is the stretch parameter; A_v and R_v parametrize the effect of interstellar dust extinction using the Cardelli-Clayton-Mathis (CCM) parametrization (Cardelli et al 1998); t_{diff}

accounts for the difference in the time of maximum of the model and the data; and z is the redshift. In other words, for Type Ia's f_j^k will become $f_j^k(\vec{\theta})$. The exact assumptions about the distribution of these parameters will be discussed below when the prior probabilities for all of the $\vec{\theta}$ parameters will be stated explicitly.

Since, in general, the exact values of each of these parameters for a given candidate are unknown, they must be marginalized. If the i^{th} measurement in filter k of the flux is F_i^k with error σ_i^k , the multi-measurement, multi-filter analog of Eqn. 4 is:

$$\mathcal{R} = \frac{\sum_{\vec{\theta}} \int_0^\infty db P(\{F_i^k\}, \{\sigma_i^k\} | \vec{\theta}, b, \text{Ia}) P(\vec{\theta}, b | \text{Ia})}{\int_0^1 d\mathbf{f}' \int_0^\infty db P(\{F_i^k\}, \{\sigma_i^k\} | \mathbf{f}', b, \text{non-Ia}) P(\mathbf{f}', b | \text{non-Ia})}. \quad (12)$$

where $\mathbf{f}' = \{f_j^k\}$, and $\int_0^1 d\mathbf{f}'$ indicates an integration over the multi-dimensional parameter space where $\sum_{k=1}^M \sum_{j=1}^N f_j^k = 1$. The denominator is not parametrized by $\vec{\theta}$ as it is not known what parameters are relevant for what we define as “anything other than SNe Ia”. Therefore, every possible distribution of light in the filters is given an equal chance.

We now address each term in Eqn. 12 in turn. $P(\{F_i^k\}, \{\sigma_i^k\} | \vec{\theta}, b, \text{Ia})$ and $P(\{F_i^k\}, \{\sigma_i^k\} | \mathbf{f}', b, \text{non-Ia})$ are the likelihoods of obtaining a set of fluxes, $\{F_i^k\}$, with uncertainties $\{\sigma_i^k\}$, for a number of measurements and filters, given that the mean number of photons are measured to be $\{f_j^k(\vec{\theta}) b\}$ and $\{f_j^k b\}$, respectively. Assuming each measurement and every filter are independent,⁴

$$P(\{F_i^k\}, \{\sigma_i^k\} | \vec{\theta}, b, \text{Ia}) = \prod_{k=1}^M \prod_{i=1}^N G(F_i^k; f_j^k(\vec{\theta}) b, \sigma_i^k). \quad (13)$$

and

$$P(\{F_i^k\}, \{\sigma_i^k\} | \{f_j^k\}, b, \text{non-Ia}) = \prod_{k=1}^M \prod_{i=1}^N G(F_i^k; f_j^k b, \sigma_i^k). \quad (14)$$

Note that, in general, the measured flux (F_i^k) and the hypothesized flux ($f_j^k b$) have different subscripts (which indicate the measurement number). This is done to emphasize the fact that it is unknown where the time of maximum of our measured light curve is relative to that of the model. This uncertainty is taken into account in one of the $\vec{\theta}$ parameters, t_{diff} .

The terms $P(\vec{\theta}, b | \text{Ia})$ and $P(\mathbf{f}', b | \text{non-Ia})$ in Eqn. 12 are prior probabilities. In particular, $P(\vec{\theta}, b | \text{Ia})$ contains the prior knowledge about the parameters $\vec{\theta}$ that describe an SN Ia. For

⁴Note that as long as the overlap between the filters is not 100%, then, without assuming anything about the underlying spectrum, any relative fraction of light is allowed between the two filters.

$P(\mathbf{f}', b|\text{non-Ia})$, \mathbf{f}' is not constrained. Likewise, parameter b is not constrained in any way for either a Type Ia or a non-Ia prior. It is therefore marginalized. Integrating over b means integrating over the total light in all the filters and all the measurements for a given candidate – *i.e.*, integrating over the observed magnitude for this measurement. Furthermore, in marginalizing b , there is an implicit assumption about the prior distribution of b – namely, that it is flat. This assumption allows us to formulate the probabilities purely in terms of color. Allowing the total light to vary measurement-by-measurement with a flat prior is arguably the lightest possible assumption one can make regarding the magnitude.

Explicitly, the priors $P(\vec{\theta}, b|\text{Ia})$ and $P(\mathbf{f}', b|\text{non-Ia})$ become:

$$P(\mathbf{f}', b|\text{non-Ia}) = \frac{1}{b_{max} - b_{min}} \delta \left(1 - \prod_{j=1}^N \sum_{k=1}^M f_j'^k \right), \quad (15)$$

since the only constraint here is that all the light fractions in different filters add up to one; and

$$P(\vec{\theta}, b|\text{Ia}) = \xi(\vec{\theta}) \frac{1}{b_{max} - b_{min}} \quad (16)$$

where $\xi(\vec{\theta})$ is the prior probability of $\vec{\theta}$.

The priors on $\vec{\theta}$ are defined similarly to those in Kuznetsova and Connolly (2007) and are briefly summarized below. The stretch parameter s follows a Gaussian distribution with a mean of $\bar{s} = 0.97$ and a width of $\delta s = 0.09$ (these values are extracted from Sullivan et al. (2006b)). The CCM parameters A_v and R_v can assume two sets of values with equal probabilities: $(A_v, R_v) = (0.0, 0.0)$ (no extinction) and $(0.2, 2.1)$ (moderate extinction). The prior probability for each choice of A_v and R_v is therefore $N_{dust} = 1/2$. The parameter accounting for the difference between the time of maximum of the data and the model, t_{diff} , has a flat prior. The measured light curve is shifted relative to a template in one day increments 1000 times and each shift is assigned an equal probability $N_{t_{diff}} = 1/1000$. means that a flat prior is assigned to t_{diff} . Finally, the redshift parameter z is assumed to be known from the supernova candidate's host galaxy, z_{gal} , with an associated uncertainty of σ_{gal} . We consider the range of redshifts from 0 to 1.7, and assume two representative possibilities for σ_{gal} , 0.005 (which might be obtained through a spectroscopic analysis of the host galaxy's spectrum) and 0.1 (obtained through a photometric analysis). Therefore,

$$\xi(\vec{\theta}) = G(s; \bar{s}, \delta s) \frac{1}{N_{dust}} \frac{1}{N_{t_{diff}}} G(z_{gal}; z, \sigma_{gal}) \quad (17)$$

Putting everything together, we obtain the full Bayes factor:

$$\mathcal{R} = \frac{\sum_{\vec{\theta}} \xi(\vec{\theta}) \int_0^\infty db \prod_{i=1}^N \prod_{k=1}^M G(F_i^k; f_i^k(\vec{\theta})b, \sigma_i^k)}{\int_0^\infty db \prod_{i=1}^N \prod_{k=1}^M \int_0^1 df_j'^k G(F_i^k; f_i^k b, \sigma_i^k) \delta \left(1 - \sum_{k=1}^M f_j'^k \right)} \quad (18)$$

where $\sum_{\vec{\theta}}$ represents the sums and integrations over the parameters in $\vec{\theta}$ (depending on whether they are discrete or continuous).

Now the calculation of Eqn. 18 requires performing $N \times M$ integrations over f_j^k in the denominator. For a large number of filters (say, ≥ 8) and many measurements, it is nearly impossible to do this calculation in a reasonable amount of time with the required precision for f_j^k without the use of techniques such as Markov Chain Monte Carlo integration methods. However, the number of integrations can be reduced to M (the number of filters) if we allow for measurement-to-measurement variations in b . That is, if we allow

$$b \rightarrow b_i, \tag{19}$$

b_i can be brought inside the product over measurements. This assumption is the equivalent of removing the knowledge that the colors between the measurements are known (or in the Poisson case, this is equivalent to having a separate multinomial for each measurement). This effectively releases the constraint on colors between measurements. Technically, the effect of this assumption should be to sweep more candidates which look less like SNe Ia into the SN Ia hypothesis, so if one’s sample contains “anomalous” candidates that very closely mimic SNe Ia one might reconsider this conjecture.

With Eqn. 19, Eqn. 18 becomes

$$\mathcal{R} = \frac{\sum_{\vec{\theta}} \xi(\vec{\theta}) \prod_{i=1}^N \int_0^\infty db_i \prod_{k=1}^M G(F_i^k; f_i^k(\vec{\theta}), \sigma_i^k)}{\prod_{i=1}^N \int_0^\infty db_i \prod_{k=1}^M \int_0^1 df_j^k G(F_i^k; f_i^k, \sigma_i^k) \delta\left(1 - \sum_{k=1}^M f_j^k\right)}. \tag{20}$$

3. Performance Studies

3.1. The Simulated Dataset

In order to check the performance of the method proposed above, we simulate a dataset closely mimicking one that could be obtained by a possible JDEM space-based mission. The mission is based on a 2-m class telescope, and is capable of taking multi-band photometric data in the wavelength range from 0.3 to 1.7 μm . Photometric data are assumed to be taken every 4 days in the observer frame, with an exposure time of 1200 seconds. Note that this study is not meant to test the performance of any particular JDEM mission; we simply test the performance of the method assuming a fairly generic, plausible JDEM.

We create a number of supernova candidates of a given type using spectral templates

from Hsiao et al (2007) for Type Ia’s, and from P. E. Nugent for non-Ia’s.⁵ The date of explosion for a given candidate is chosen randomly within the confines of a 3 year mission timeline, and supernova candidate properties are generated according to the probability distribution functions in $\xi(\vec{\theta})$ (see Eqn. 17). The supernova light curves are then realized using a simple aperture exposure time calculator. We generate supernova candidates of types Ia, Ibc, II-P, and IIn. We assume that the intrinsic rest-frame B -band magnitudes follow a Gaussian distribution, with the mean and standard deviations obtained from Richardson et al. (2002). In particular, the mean and standard deviation are taken to be -19.05 ± 0.30 mags. for Type Ia’s; -17.27 ± 1.30 mags. for Type Ibc’s; -19.05 ± 0.92 mags. for Type IIn’s and -16.64 ± 1.12 mags. for Type II-P’s. We also generate “anomalous” objects by creating fake unimodal light curves (light curves that rise and fall with a single maximum, but are otherwise random). These light curves are assigned 1% errors in each broadband filter considered.

To get a better feel for the simulated dataset, Fig. 1 shows the signal-to-noise ratios at maximum light as a function of redshift for the simulated SNe Ia in the filter that most closely matches the rest-frame B -band.

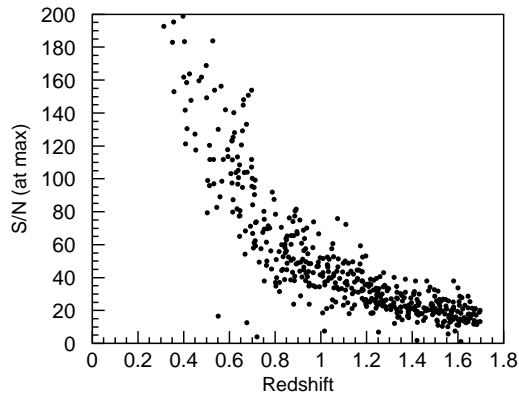


Fig. 1.— Distribution of the signal-to-noise ratios at maximum light as a function of redshift for the simulated SNe Ia, in the filter that most closely matches the rest-frame B -band.

Once the light curves are simulated, we select a subset of them in a limited number of broadband filters. The chosen filters must include those that most closely match the

⁵See http://supernova.lbl.gov/~nugent/nugent_templates.html.

rest-frame B - and V - bands for a given candidate. The reason why we place a particular emphasis on these bands is because they correspond to a wavelength range where SNe Ia are particularly well modeled. To limit the computational time, we only consider 50 consecutive photometric measurements (the actual available number of measurements varies evenly from 0 to over 350). We also require that there be at least one measurement with a signal-to-noise ratio > 5 in the filter most closely corresponding to the rest-frame B -band for a given candidate. Any space-based dark energy mission that extends to at least a year and uses SNe Ia as a dark energy probe will satisfy these requirements (in fact, every JDEM mission currently on the market does).

3.2. Results

A number of tests are used to check the performance of the method. First, we calculate the Bayes factor, \mathcal{R} (Eqn. 20), for a sample of simulated SNe Ia and a sample containing unimodal “fake” light curves. The unimodal light curves for a given “object” peak at the same time in all the filter bands. To give a sense of their color distribution, Fig. 2 shows the fake objects’ colors for the 3 lowest wavelength filters bands (the first filter covers the range of 0.32-0.47 μm ; the second, 0.41-0.56 μm ; and the third, 0.49-0.68 μm). This test

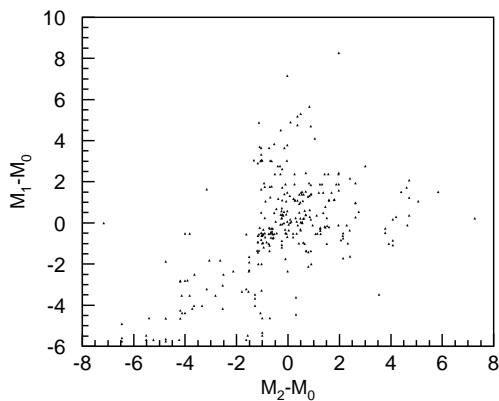


Fig. 2.— The distribution of colors for the fake unimodal data. M_i is the magnitude in filter i (filter 0 covers the range of 0.32-0.47 μm ; filter 1, 0.41-0.56 μm ; and filter 2, 0.49-0.68 μm).

allows us to test the discrimination between SNe Ia and objects that are not supernovae of

any kind. Figure 3 shows that $\log\mathcal{R}$ is predominantly positive for SNe Ia and negative for the random, unimodal data, meaning that $\mathcal{R} < 1$. This means that the method behaves as expected, discriminating between random data and true supernovae 100% of the time.

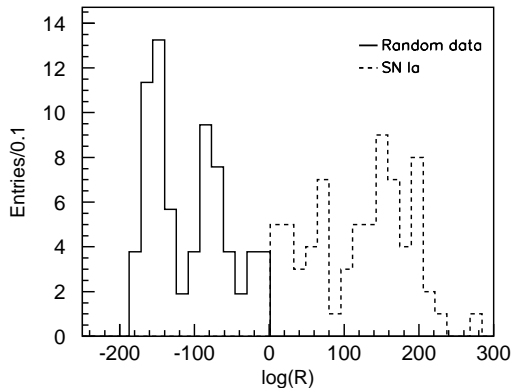


Fig. 3.— Distributions of $\log\mathcal{R}$ for random unimodal data (solid line) and SN Ia’s (filled histogram). The two histograms have been normalized to the same area for an easier shape comparison.

We also compute the Bayes factor for a sample of simulated Type Ibc’s, Type II-P’s, and Type IIn’s. Note that we do not have to include any information about the expected light curves for Type Ibc’s, Type IIn’s, or Type II-P’s to compute \mathcal{R} . Figure 4 shows the comparison of $\log\mathcal{R}$ for the case of measurements in 2 filters (left column) and 4 filters (right column). We consider the case of a 0.1 error on the redshifts (top row) and a 0.005 error on the redshift (bottom row). For this comparison, we assume that the errors on the supernova fluxes are realistic (that is what a JDEM mission described above would be expected to obtain). Several interesting conclusions can be drawn from Fig. 4. First, it is apparent that the method does discriminate between SNe Ia and the other types, although $\log\mathcal{R}$ tend to be larger than 0 (so that $\mathcal{R} > 1$) because SNe Ia are far more similar to other supernovae than they are to anything else. It should be noted that the values of \mathcal{R} tends to be quite large. This is due to our use of a large number of measurements (~ 50) in a number of filters, which ensures that a candidate is either very much identified as an SN Ia-like candidate or not. Second, as expected, the discrimination between SN Ia’s and non-Ia’s increases with more information (4 filters vs. 2 filters) and/or with better prior knowledge (*i.e.*, smaller errors on the measured redshift). Third, the discrimination is somewhat worse at high redshifts ($> \sim 1$), as we move into a domain of less precise data and less certain models; but it is

still good enough for \mathcal{R} to be used as a first-pass SN Ia classifier. Additionally, at least some plausible JDEMs “sculpt” their expected SNe Ia distribution so that it peaks at $z \sim 0.7$ (Aldering et al. 2004).

One might ask how \mathcal{R} would be affected if the templates used had incorrect colors for the SN Ia hypothesis. In order to answer this question, we generated SN Ia candidates with $(A_v, R_v) = (0.2, 2.1)$ but use only the no-extinction templates when calculating \mathcal{R} . Figure 5 shows the distributions of \mathcal{R} for the cases where the extinction parameters in the data and templates are matched and mis-matched. As expected, \mathcal{R} decreases when the extinction in the templates does not match that in the data; that is, the SNe Ia look more similar to non-SNe Ia.

We further check the behavior of \mathcal{R} by varying the errors on the fluxes of the simulated SNe Ia to ensure that \mathcal{R} changes in the right direction. This check, always a good idea for a newly introduced statistic, is particularly important for this Bayes factor, which makes use of improper priors that can lead to non-intuitive behavior (Berger and Pericchi (2001)). Figure 6 shows the distribution of $\log \mathcal{R}$ for the “nominal” flux errors and for flux errors artificially increased and decreased by a factor of 2. Increasing the flux errors shifts the distribution to the left (*i.e.*, the discrimination power decreases), while decreasing the flux errors shifts it to the right (*i.e.*, the discrimination power increases). This is the expected behavior for a correctly computed \mathcal{R} .

3.3. Including Prior Knowledge on Non-Ia Supernova Types

So far, we have assumed no prior knowledge of SNe models that may contribute to the set of observed non-SNe Ia. We showed that the Bayes factor described above is capable of discriminating between SNe Ia and non-SNe Ia as well as random unimodal light curves that mimic anomalous candidates. This discrimination, which does not require either the knowledge of a complete set of objects that can mimic an SN Ia signal or the knowledge of the possible behavior of anomalous non-supernova objects that can contaminate an SN Ia signal, is good. As Fig. 4 shows, we could simply define a polynomial cut on \mathcal{R} as a function of \mathcal{R} and have a very good discriminant.

However, one might be interested in considering a Bayes factor for which all *known* non-SN Ia candidates would have $\mathcal{R} < 1$. First, it is simply better to have a \mathcal{R} that behaves intuitively. Second, it is obvious that including more prior knowledge (*i.e.*, the knowledge of what can potentially mimic an SN Ia signal), can only sharpen the discrimination between SNe Ia and non-SNe Ia. Third, and more importantly, it is a good idea to have a discriminant

such that $\mathcal{R} < 1$ when the candidate is more likely to be an SN Ia than not, and $\mathcal{R} > 1$ otherwise. This allows one to use a formalism similar to that described in Wald (1945, 1947) in order to set thresholds on \mathcal{R} with meaningful, pre-determined Type I and II error rates.

Explicitly including the knowledge about the behavior of non-SNe Ia into Eqn. 1, we define:

$$\mathcal{R}' = \frac{P(\text{Phot}|\text{Ia})}{P(\text{Phot}|\text{II-P})P(\text{II-P}|\text{non-Ia}) + P(\text{Phot}|\text{Ibc})P(\text{Ibc}|\text{non-Ia}) + P(\text{Phot}|\text{IIIn})P(\text{IIIn}|\text{non-Ia}) + P(\text{Phot}|\text{anything})P(\text{anything}|\text{non-Ia})}, \quad (21)$$

where the denominator now accounts for the probability that the observed photometry can come from a Type II-P supernova, $P(\text{Phot}|\text{II-P})$; a Type Ibc supernova, $P(\text{Phot}|\text{Ibc})$; or from a Type IIIn supernova, $P(\text{Phot}|\text{IIIn})$. $P(\text{Phot}|\text{anything})$ is equivalent to the denominator in Eqn. 20. Note that the prior terms in Eqn. 21 are such that

$$P(\text{II-P}|\text{non-Ia}) = P(\text{Ibc}|\text{non-Ia}) = P(\text{IIIn}|\text{non-Ia}) = P(\text{anything}|\text{non-Ia}) = \frac{1}{4} \quad (22)$$

In other words, there is an equal probability of measuring a Type Ia supernova, a Type Ibc supernova, a Type II-P supernova or some other object denoted as “anything”. It is of course trivial to introduce relative rates if they are known; however, it is immaterial for our purpose, which is demonstrating the performance of the method.

The non-Type Ia probabilities are calculated in exactly the same way as those for Type Ia’s, using the available models for the corresponding types. The distribution of $\log\mathcal{R}'$ vs. redshift is shown in Fig. 7, for the case of 2 filters (left column) and 4 (right column) filters with 0.005 flux errors (bottom row), and 0.1 errors (top row) on the redshift. Randomly generated, uni-modal data all have large negative values $\log(\mathcal{R})$ ’s that dwarf the scales on these figures. The errors on the flux are those expected for a JDEM mission described above. Compared Fig. 7 to Fig. 4, it is clear that not only has the discrimination between SNe Ia and everything else increased, but also the SNe Ia generally have $\log(\mathcal{R}') > 0$ and other candidates have $\log(\mathcal{R}') < 0$. This is the desired behavior for \mathcal{R}' .

A number of features of Fig. 7 are similar to those apparent in Fig. 4, such as the increase in the discrimination power when more and/or better information becomes available.

3.4. Dangers of a Finite Set Assumption

As we explained in Section 1, existing Bayesian-based methods of supernova classification assume a finite set of possible objects that can mimic an SN Ia signal. To demonstrate the danger of this limiting assumption, we use our unimodal fake light curves and calculate Bayes factors defined as:

$$R_{Ia} = \frac{P(\text{Phot}|\text{Ia})P(\text{Ia})}{P(\text{Phot}|\text{Ibc})P(\text{Ibc}|\text{non-Ia}) + P(\text{Phot}|\text{II-P})P(\text{II-P}|\text{non-Ia}) + P(\text{Phot}|\text{IIIn})P(\text{IIIn}|\text{non-Ia})} \quad (23)$$

and

$$R_{II-P} = \frac{P(\text{Phot}|\text{II-P})P(\text{II-P})}{P(\text{Phot}|\text{Ibc})P(\text{Ibc}|\text{non-Ia}) + P(\text{Phot}|\text{Ia})P(\text{Ia}|\text{non-Ia}) + P(\text{Phot}|\text{IIIn})P(\text{IIIn}|\text{non-Ia})} \quad (24)$$

Figure 8 shows that the fake objects can be mis-identified as supernovae of types other than ia (in particular, as Type II-P’s), as well as SNe Ia: there are candidates with $R_{Ia} > 1$. This further demonstrates the need for a general formalism that is capable of discriminating a certain type of supernovae (most often Type Ia’s) from *anything else*.

4. Summary

We have introduced a new photometric supernova classification scheme that uses a Bayes factor based on color. The proposed method is fundamentally different from previous supernova classification methods including our own (Kuznetsova and Connolly 2007) because it allows one to discriminate not only between supernovae of different types but also between supernovae and “anomalous” objects. It has a number of definite advantages over many existing techniques for selecting SNe Ia out of a pool of supernova candidates. The main one is that it does not pre-suppose any prior knowledge about the objects that could potentially mimic a Type Ia signal. It can thus be used as a very good first-pass Type Ia classifier. With the current poor knowledge of the behavior of non-Type Ia supernovae, especially at high redshifts, and the expected dramatic increase in the discoveries of new, as yet unknown classes of transient astronomical objects, this feature of the method will be invaluable for future supernova surveys. This is not, however, an excuse not to obtain as much information about non-Type Ia supernovae as one possibly can, as evidenced by the advantage of computing \mathcal{R}' , which includes information about the light curves of Type Ia, Ibc, IIIn, and II-P supernovae (obviously, more information means a better performance).

Another principal advantage of the proposed method is that if the Bayes factor described in Section 3.2 is used as a discriminant, the only supernova models that are required are those for SNe Ia, which are the best studied and most complete of all the supernova types. One may argue that the same is true for a χ^2 -based method. However, χ^2 methods suffer from a number of problems described in Section 1, the least of which is that for the case of data with large uncertainties a given supernova candidate will appear to agree with many possible supernova type hypotheses, with one necessarily giving the “best” χ^2 (however insignificant the difference between this best χ^2 and the χ^2 ’s from the other fits may be). The Bayes factor, on the other hand, would be of order 1, reflecting ambiguity between the hypothesis that the candidate is an SN Ia and that it is anything else.

Finally, as it is a Bayesian approach, it accounts for all systematic and statistical uncertainties of the measurements in all their forms.

We demonstrated the method on a simulated dataset expected from a possible future large-scale space-based JDEM. It must be noted that most existing data sets include primarily SNe Ia; at the present time large datasets with exotic supernovae that would allow us to perform a statistically meaningful study of the method’s performance are not available (although we are planning on exploring the application of this method to an existing dataset of non-standard supernovae in a future publication). Nevertheless, a number of interesting conclusions can be drawn from the simulation studies described above:

- The method provides a 100% discrimination between SNe Ia and unimodal random data. This is encouraging, since many transient objects (such as active galactic nuclei) that are sometimes mistaken for supernovae tend to have a rather erratic behavior, deviating far more from an SN Ia light curve than the simple random unimodal data. More fundamentally, the discrimination also shows that \mathcal{R} and \mathcal{R}' behave as expected.
- The discrimination between Type Ia’s and other supernova types is near 100% at low redshifts when calculating $\log\mathcal{R}$. At higher redshifts, Fig. 4 shows that that a “straight line” cut on $\log\mathcal{R}$ would render a reasonably high purity and efficiency for SNe Ia. Alternatively, one could invent a more sophisticated cut (*e.g.*, a polynomial). The discrimination is practically 100% at all redshifts if $\log\mathcal{R}'$ is used (*i.e.*, when information about the behavior of Type II-P, Type Ibc, and Type IIn supernovae is included in calculating $P(\text{Phot}|\text{non-Ia})$).
- The method performs better when more information about the data becomes available. For example, the discrimination between SNe Ia and non-SNe Ia increases dramatically when the number of filters goes from 2 to 4. This shows that, despite the use of improper priors, the Bayes factor behaves properly.
- Increasing the precision on the redshift of the supernova candidates also improves the discrimination between Type Ia’s and non-SNe Ia.
- It is important that the data and the models used have a good match in terms of expected colors. For example, if the extinction assumptions in the data are different from those in the models, real SNe Ia are more likely to be classified as anomalous objects.
- Figures 4 and 7 indicate that there is sufficient separation between various supernova candidates, so that this method could be used for classification in the strict sense of giving a type (*e.g.*, a Type Ia, a Type Ibc, *etc.*) to each candidate, along with some associated probability.

The method does not make use of magnitudes. One might see this as an advantage if one does not entirely trust the distribution of intrinsic magnitudes. Insertion of absolute magnitudes is possible, but the formulation of \mathcal{R} (\mathcal{R}') becomes inelegant and requires knowledge of an upper limit of intrinsic magnitudes of anomalous candidates that, by definition, have not been observed. It is indeed fortunate that color alone is sufficient to classify supernovae, allowing for a simple and elegant solution for \mathcal{R} (\mathcal{R}').

There is another reason not to include magnitudes into the formalism, at least at the present time. The distributions of the intrinsic magnitudes for non-SNe Ia are at the moment rather poorly known (Richardson et al. 2002). In fact, very little is known about high-redshift non-SNe Ia (for example, Dahlen et al. (2008) remains the only measurement of the non-SNe Ia rates to redshifts of ~ 1). There exists a very real need to measure the properties of non-SNe Ia supernovae with more precision, a task that is ideally suited for existing and planned large-scale supernova surveys.

It is also important to note the computational challenges in calculating \mathcal{R} (\mathcal{R}'). The number of filters used in the calculation depends on the precision needed for the integration of $\{f_j^k\}$. It was found that for 4 filters about 150 integration points for f_j^k were needed for a precise calculation of the denominator, $P(\text{Phot}|\text{non-Ia})$. This was found by increasing the number of integration points until the value of the denominator became stable.

In order to complete the computations in a reasonable amount of time, it was necessary to perform the calculations of the Bayes factor for many candidates in parallel. The computational feasibility also depended on approximating $b \rightarrow b_i$, as was discussed in Section 2.2, so as to reduce the number of integrations from $N \times M$ (where N is the number of flux measurements and M is the number of filters) to M . This effectively required that we gave up information about the supernova colors measured in the various filters and allowed the colors to vary measurement-to-measurement. One might be concerned that this approximation would in fact allow for a greater diversity in what is considered an SN Ia – that is, in general objects would have a greater chance of faking an SN Ia. However, in our studies we found that, at least with the level of precision of the models and simulated data used, the calculated Bayes factor provided desired discrimination between SNe Ia and other objects, leading us to believe that this is not a significant effect.

We also point out that our proposed technique is general enough to be used for objects other than supernovae. For example, Richards et al. (2004) propose a Bayesian classifier to differentiate quasars and stars, defined as:

$$P(\text{star}|x) = \frac{P(x|\text{star})P(\text{star})}{P(x|\text{star})P(\text{star}) + P(x|\text{quasar})P(\text{quasar})} \quad (25)$$

where x is a candidate's position in a 4-dimensional color space. Although the likelihoods,

$P(x|\text{star})$ and $P(x|\text{quasar})$ are obtained using a training sample derived from real data, new data inevitably bring new objects which could be accounted for by inserting an “anomaly” term similar to $P(\text{Phot}|\text{anything})P(\text{anything})$ in Eqn. 21. This term would sweep up those objects that do not conform to the existing models for quasars or stars in the same way that $P(\text{Phot}|\text{anything})P(\text{anything})$ accounts for anomalous supernova candidates; its exact form would depend on the nature of the statistical fluctuations in the data.

4.1. \mathcal{R} Used in the Context of an SN Ia Trigger

Note that while our method relies only on photometric information about supernovae, some proposed future space-based dark energy missions do plan on obtaining the spectrum of every candidate. One possible scenario would be to obtain the spectrum of a candidate provided that a) it is highly likely to be an SN Ia, and b) it is at its peak brightness. In this case it is necessary to have reliable means to be able to tell whether or not a given candidate is most likely an SN Ia or not based on its pre-maximum photometric measurements alone. In other words, it is important to have a *trigger* mechanism that would photometrically select candidates for possible spectroscopic follow-up. Our proposed Bayes factor can be simply modified to allow for such a usage. Assuming that one wants to trigger on supernovae before maximum brightness, the Bayes factor becomes:

$$\mathcal{R}'' = \frac{P(\text{Phot}|\text{Ia pre-max})}{P(\text{Phot}|\text{Ia post-max}) + P(P(\text{Phot}|\text{II-P})P(\text{II-P}|\text{non-Ia}) + P(\text{Phot}|\text{Ibc})P(\text{Ibc}|\text{non-Ia}) + P(\text{Phot}|\text{anything})P(\text{anything}|\text{non-Ia})}, \quad (26)$$

where $P(\text{Phot}|\text{Ia pre-max})$ would only include supernova models with points before maximum light, while $P(\text{Phot}|\text{Ia post-max})$ would only include those with points after maximum light. After calculating this Bayes factor, a cut would be made at, say, $R'' > 1$ to choose those candidates that are likely to be SNe Ia and that have not yet reached maximum.

Better still, one could use a *sequential analysis* technique (Wald 1945, 1947) to minimize the data required to make this decision while simultaneously controlling identification errors. This is done by setting thresholds on \mathcal{R}'' based on pre-selected Type I and Type II error rates. The demonstration of the performance of a sequential analysis-based approach will be the subject of a future publication.

5. Acknowledgments

NC gratefully acknowledges support from a Cottrell College Science Award from the Research Corporation and from NSF RUI award #0806877, as well as from Hamilton College. BC is partially supported by grant #DE-FG02-95ER40893 from the U.S. Department of Energy. We thank Steve Young at Hamilton College for computer technical support.

REFERENCES

- Aldering, G., *et al.*, 2004, submitted to PASP [preprint astro-ph/0405232]
- Barbary, K., *et al.*, 2009, ApJ, 690, 2, 1358
- Baron, E., Nugent, P., Branch, D., Hauschildt, P., 2004, ApJ, 616, 91
- Berger, J., and Pericchi, L., 2001, *Model Selection*, in Institute of Mathematical Statistics Lecture Notes, ed. P. Lahiri, Monograph Series Vol. 38
- Cardelli, J. A., Clayton, G. C., and Mathis, J. S., 1998, ApJ 329, L33
- Conley, A., *et al.*, 2008, ApJ, 681, 482.
- Dahlen, T., *et al.*, 2008, ApJ, 681, 462
- Edwards, A. W. F., 1992, *Likelihood*, Johns Hopkins University Press
- Hamuy, M. & Pinto, P. A. 2002, ApJ, 566, L63
- Hsiao, E. Y., *et al.*, 2007, ApJ, 663, 1187
- Gradshteyn, I. S., & Ryzhik, I. M., 2000, *Table of Integrals, Series and Products*, Edited by A. Jeffrey and D. Zwillinger, Academic Press, New York, 6th edition
- Guy, J. *et al.*, 2007, A&A, 466, 11
- Jha, S., Riess, A. G., & Kirshner, R. P., 2007, ApJ, 659, 122
- Jaynes, E. T., and Bretthorst, G. L. (Eds), 2003, *Probability Theory: The Logic of Science*, Cambridge University Press
- Jeffreys, H., 1961, *Theory of Probability*, Third Edition, Oxford University Press
- Johnson, B., and Crotts, A., 2006, AJ, 132, 756
- Kuznetsova, N., and Connolly, B. M., 2007, ApJ, 659, 530
- Nugent, P. *et al.* 2006, ApJ, 645, 841
- Perlmutter, S., *et al.* 1997, ApJ, 483, 565
- Poznanski, D., *et al.*, 2002, PASP, 114, 833
- Poznanski, D., Maoz, D., and Gal-Yam, A., 2007, AJ, 134, 1285

- Poznanski, D., *et al.*, 2009, ApJ, 694, 2, 1067
- Riess, A. G., *et al.*, 2004, ApJ, 600, L163
- Richards, G. T., *et al.* 2004, Astrophys.J.Suppl., 155, 257
- Richardson, D.,*et al.* 2002, AJ, 123, 745
- Sellke, T., Bayarri, M. J., and Berger, J. O., 2001, *The American Statistician*, 55, 1, 62
- Sullivan, M., *et al.*, 2006, AJ, 131, 960
- Sullivan, M., *et al.* 2006, ApJ, 648, 868
- Wald, A. 1945, Ann. Math. Stat., 16, 117
- . 1947, *Sequential Analysis*, John Wiley and Sons

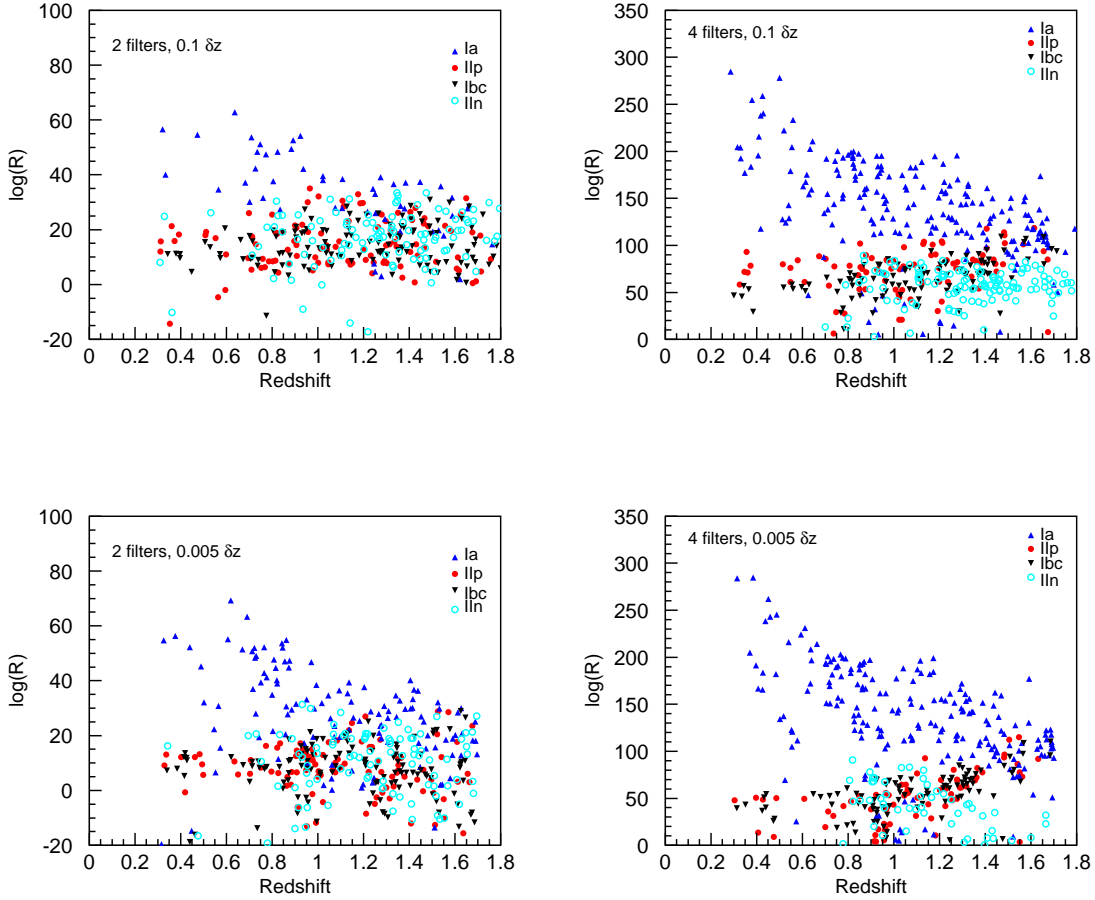


Fig. 4.— Distributions of $\log\mathcal{R}$ vs. redshift for Type Ia's (upward turned triangles), Type Ibc's (downward turned triangles), Type II-P's (filled circles) and Type IIn's (open circles), with a 0.1 error on the candidate redshifts (top row) and a 0.005 candidate redshifts (bottom row), for 2 filters (left plots) and 4 filters (right plots). The unimodal random data are not over-plotted on these figures because they all have large negative values $\log(\mathcal{R})$'s that dwarf the y -axis scales.

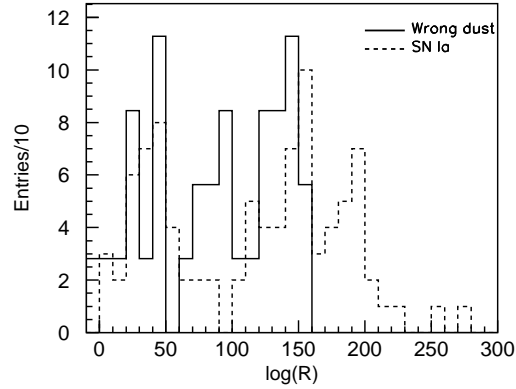


Fig. 5.— The distributions of \mathcal{R} for the case of the extinction mis-match between the data and the templates (solid line), and the case of the matching extinction assumptions for the data and the templates (dashed line). The mis-matching case clearly results in a worse discrimination, making SNe Ia look more like “anomalous” objects; this is because the extinction in the data is not accounted for in the set of templates used to define an SN Ia.

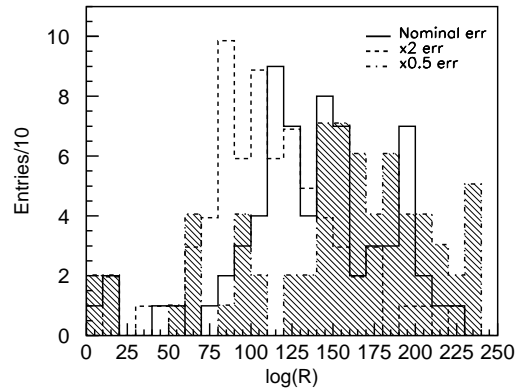


Fig. 6.— Distributions of $\log \mathcal{R}$ for simulated Type Ia candidates for nominal flux errors (solid line), flux errors increased by a factor of 2 (dashed line), and flux errors decreased by a factor of 2 (dot-dashed line, filled histogram). The histograms have been normalized to the same area to aid in the comparison of their shapes.

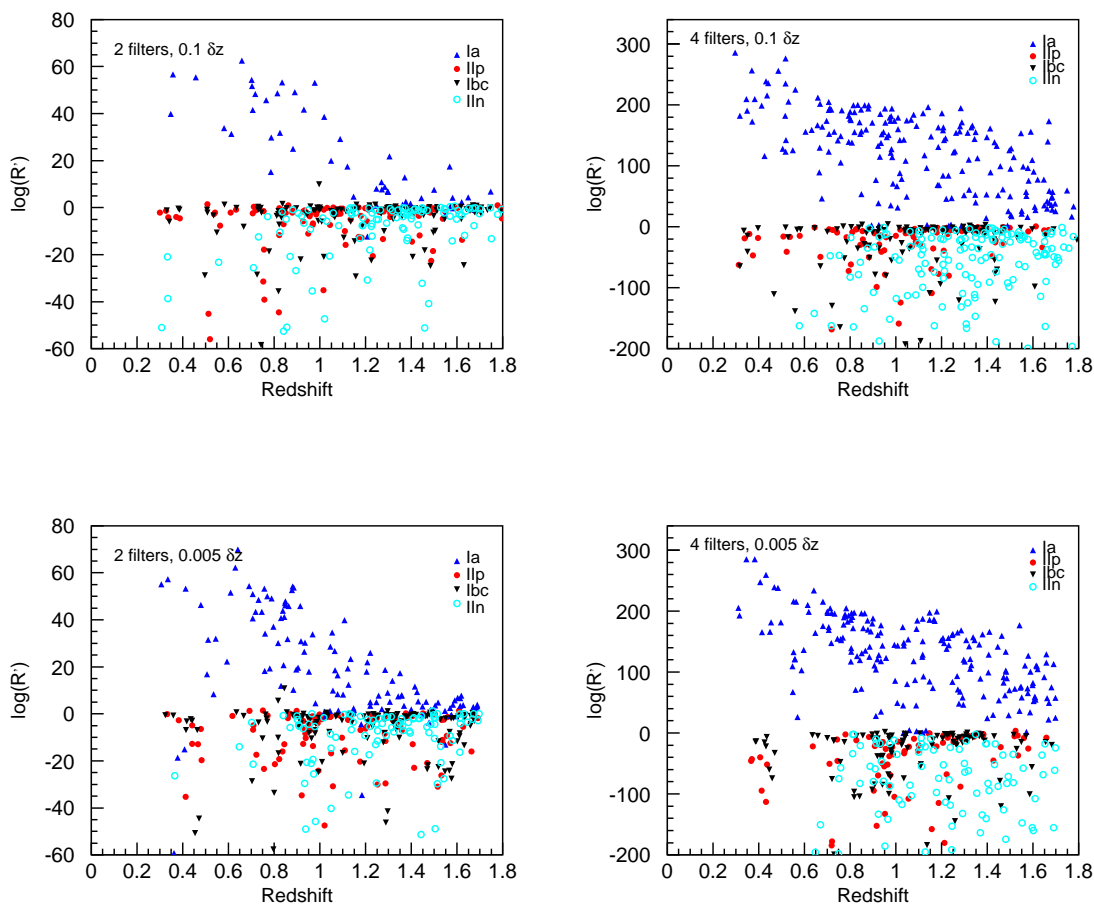


Fig. 7.— Distributions of $\log \mathcal{R}'$ vs. redshift for Type Ia’s (upward turned triangles), Type IIbc’s (downward turned triangles), Type II-P’s (filled circles) and Type IIin’s (open circles), with a 0.1 error on the candidate redshifts (top row) and a 0.005 error on the candidate redshifts (bottom row), for 2 filters (left plots) and 4 filters (right plots).

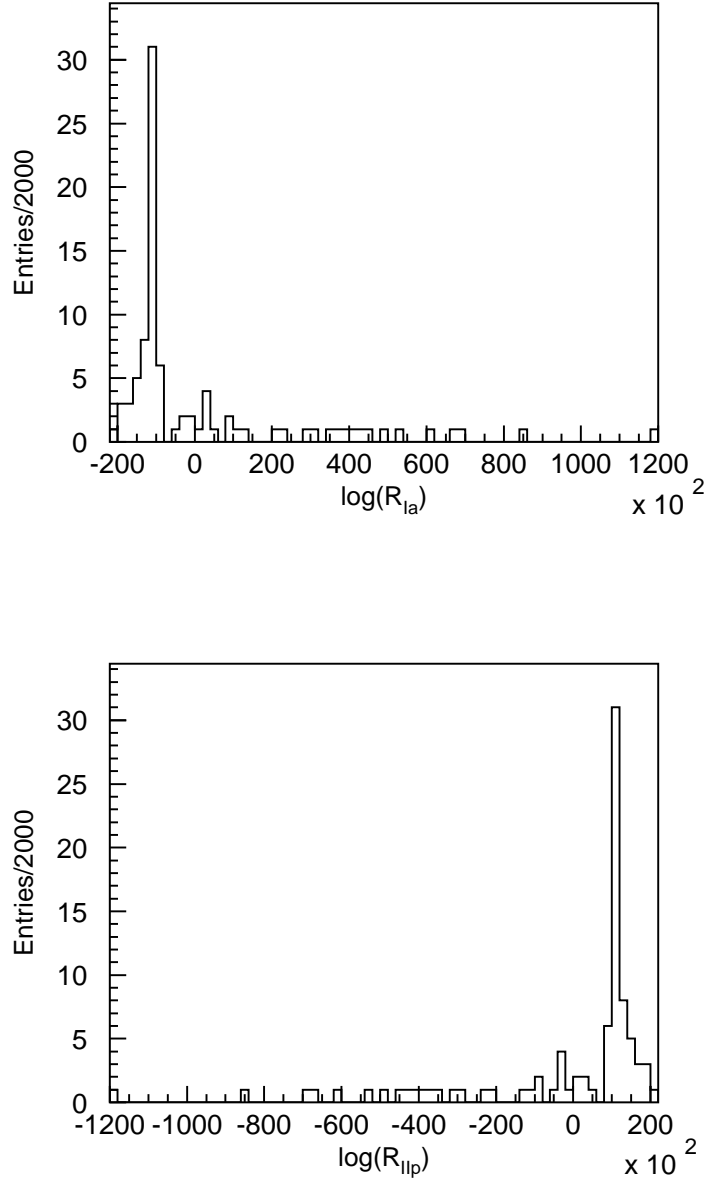


Fig. 8.— The distributions of $\log R_{Ia}$ (top) and $\log R_{II-P}$ (bottom) for a set of unimodal random light curves.